Environmentally friendly approach to the synthesis of monodisperse and bright blue emitting $Cd_{0.15}Zn_{0.85}S$ quantum dots

Anastasia Iakovleva[1], Liudmila Loghina[1], Zuzana Olmrova Zmrhalova[2,1], Jan Mistrik[3,1], Petr Svec[4], Stanislav Slang[1], Karel Palka[4,1] and Miroslav Vlcek[1]

[1]Center of Materials and Nanotechnologies, Faculty of Chemical Technology, University of Pardubice, nam. Cs. legii 565, Pardubice 53002, Czech Republic
[2]Joint Laboratory of Solid State Chemistry, Faculty of Chemical Technology, University of Pardubice, Studentska 84, Pardubice 53210, Czech Republic
[3]Institute of Applied Physics and Mathematics, Faculty of Chemical Technology, University of Pardubice, Studentska 95, Pardubice 53210, Czech Republic
[4]Department of General and Inorganic Chemistry, Faculty of Chemical Technology, University of Pardubice, Studentska 95, Pardubice 53210, Czech Republic

E-mail: Liudmila.Loghina@upce.cz

Abstract

Nucleation and growth of quantum dots (QDs) in solution are mainly controlled by the kinetic and thermal modes of the reaction process. By influencing any of them, the properties of the final nanocrystals can be tuned. The influences of temperature and chemical nature of starting materials on nucleation and, as a consequence, on the structure and optical properties of $Cd_{0.15}Zn_{0.85}S$ QDs have been systematically investigated by one-pot and hot-injection methods. All reactions were performed in organic disperse medium using N,N′-disubstituted and N,N′,N′-trisubstituted thioureas (TU) as a new sources of sulfur. In addition to environmental friendliness, each of them has a number of unique chemical properties. The effect of the substituents' nature in thioureas on the morphology, size and optical properties of synthesized QDs has been studied. The strong correlation between the metal ratios taken to the reaction and elemental analysis (EDS) results for all obtained $Cd_{0.15}Zn_{0.85}S$ QDs was found. However, prepared nanomaterials have different size (2.9 – 4.6 nm) and morphology. The optical features have also changed under the various thermal conditions. Especially, the changes in the photoluminescence spectra of QDs synthesized with different thioureas are noticeable. Highly photoluminescent (photoluminescence quantum yield PL QY up to 67 %), morphologically and structurally homogeneous blue-emitting $Cd_{0.15}Zn_{0.85}S$ QDs were obtained.

Keywords: quantum dots, substituted thioureas, semiconductors

1. Introduction

In recent years semiconductor quantum dots (QDs) are widely used in various optoelectronic systems, such as light emitting diodes and flat light emitting panels [1, 2], lasers, solar cells and photoelectric converters [3, 4], FRET (Fluorescence Resonance Energy Transfer) based sensors [5], as biological markers for biomedical and environmental applications [6 – 8] *i.e.* wherever is needed to have variable and tunable optical properties. Also, semiconductor QDs are quite successfully used today as photocatalysts in the reactions of photocatalytic reduction of aromatic nitro compounds [9], the formation of carbon disulfide [10] and reductive dehalogenation [11].

Since the last decade ternary alloyed CdZnS QDs have attracted great attention due to their composition dependent optoelectronic properties. Recently Mandal *et al.* has reported the efficient resonance energy transfer-based photophysical interaction between CdZnS QDs and porphyrin-based ligand as one of the possible applications of these composites as biosensors [12]. Furthermore, blue ZnCdS/$Cd_xZn_{1-x}S$/ZnS light-emitting devices with a high external quantum efficiency (EQE) were presented by Wang and co-workers [13].

Optical properties, such as the intensity and the position of photoluminescence signal in the wavelength scale, the position of the first exciton maximum in the absorbance spectrum and, therefore, the bandgap E_g of the nanomaterial directly depends on the composition and size of the QDs [14].

Up to date, there are many synthetic protocols providing nanomaterials [15]. Among them, the most common method is a preparation in the liquid dispersion phase, which is a colloidal synthesis in an organic medium with the participation of surfactants. Here, one should distinguish the hot-injection method and the one-pot method, each of them exhibiting their own advantages. For the synthesis of CdZnS QDs, both approaches can be used. The main advantage of the hot-injection method is immediate nucleation and uniform growth of crystals and, consequently, the homogeneity of the nanoparticles and the minimum of defects in the crystal. Alloyed $Zn_xCd_{1-x}S$ nanocrystals (2.4 nm – 4.0 nm, PL QY 25 – 50 %) with the hexagonal structure were prepared by hot-injection method at 300 °C within excess of oleic acid [16]. Wang *et al.* [17] used different ratios of manganese for doping of CdZnS QDs (up to 8.0 nm for core/shell QDs) prepared by hot-injection method to improve the stability of nanomaterials and to enhance their PL QY up to 48.8 %.

The one-pot method is characterized by simplicity of the procedure, the best thermoregulation, stable and consistent nucleation when compared to other synthetic methods. In our opinion, one-pot method can be quite attractive for the large-scale industrial synthesis of such nanomaterials. Application of the mixture sulfur/2,2'-dithiobisbenzothiazole as a source of sulfur in the $Zn_xCd_{1-x}S$ QDs synthesis was presented *via* a non-injection one-pot approach [18]. The synthesis of QDs (QDs sizes 3.5 – 4.2 nm with corresponding PL QY up to 23%) for was performed in 1-octadecene (ODE) at 240 °C. Light-emitting diodes (LEDs) fabrication on the base of $Cd_xZn_{1-x}S$ QDs prepared by one-pot method in liquid disperse medium was presented by Jin and co-workers [19]. In addition to all previously discussed factors, which affect the properties of nanomaterials, the temperature has a great influence on the synthesis, independently on the sulfur source's nature.

In this paper, we present a study of the temperature impact on the synthesis of $Cd_{0.15}Zn_{0.85}S$ QDs using new sulfur sources. The influence of the synthesis temperature on the nucleation and growth of QDs, and consequently on the morphology, structure, and optical properties of the obtained nanomaterials, was studied by two synthetic approaches. A comparison of the hot-injection and one-pot synthetic methods studied in the temperature range 220 - 300 °C was carried out using (Z)-1-(octadec-9-enyl)-3-phenylthiourea as a source of sulfur. This N,N′-disubstituted thiourea was recently studied [20] for an explanation of chemical processes taking place in the synthesis of QDs. In addition to that, we present research of the substituents nature influence on the structural and optical properties of QDs. For this purpose, we synthesized substituted thioureas from the corresponding isothiocyanates and amines. To the best of our knowledge, the synthesized thioureas have not been previously used for the

preparation of ternary QDs. The resulting $Cd_{0.15}Zn_{0.85}S$ QDs exhibited the narrow PL emission signals with a full width at half maximum (FWHM) to 32 nm and high PL QY (up to 67 %).

2. Experimental section

2.1 Materials

Cadmium oxide (CdO, 99.99 %), zinc oxide (ZnO, 99 %), oleylamine (OAm, technical grade, 70 %), linoleic acid (LA, technical grade, 60-74 %), 1-octadecene (ODE, technical grade, 90 %), phenyl isothiocyanate (98 %), allyl isothiocyanate (95 %), carbon disulfide (CS_2, 99 %) isobutylamine (99 %), morpholine (99 %), aniline (99.5 %), 2,4,6-trichloro-1,3,5-triazine (TCT, 99 %) chloroform-d ($CDCl_3$, 99.8 atom % D) and silica gel (high-purity grade, pore size 60 Å, 230 - 400 mesh particle size) were purchased from Sigma-Aldrich and used without further purification. Sodium hydroxide (NaOH, p.a.), hydrochloric acid (HCl, 35 %), potassium carbonate (K_2CO_3, p.a.) and solvents were purchased from Fisher Scientific and used for purification of organic precursors and QDs. Syntheses of QDs were carried out using standard Schlenk techniques under an Ar atmosphere.

2.2 Synthesis of di- and trisubstituted thioureas

2.2.1 Synthesis of isobutyl isothiocyanate.

In a typical synthesis, potassium carbonate (K_2CO_3, 0.055 mol, 7.59 g) and 30 ml of distilled water were charged in a three-necked round bottom flask equipped with a magnetic stirrer, thermometer, reflux condenser, and a dropping funnel. The mixture was stirred until complete dissolution followed by the addition of isobutylamine (*i*-$BuNH_2$, 0.05 mol, 3.66 g). Subsequently, carbon disulfide (CS_2, 0.1 mol, 7.61 g) was slowly added dropwise to the reaction mixture at room temperature (slightly exothermic). After complete addition, the reaction mixture was stirred at room temperature for three hours. The complete conversion was controlled by thin-layer chromatography (TLC) and GC/MS methods. The reaction mixture was then cooled to 0 °C and TCT solution (0.025 mol, 4.61 g) in 20 ml of CH_2Cl_2 was added dropwise under vigorous stirring, while precipitation was observed. Afterwards, the reaction mixture was stirred for an additional hour. Then 10 % aqueous NaOH solution was added in small portions to pH > 11, causing the precipitate to dissolve completely. The resulting mixture was transferred to the separation funnel followed by extraction with methylene chloride (CH_2Cl_2, 3 x 20 ml). The combined organic extracts were consequently washed with 1 % HCl aqueous solution, brine and further dried over anhydrous Na_2SO_4. The solvent was removed on a rotary evaporator and the residue was purified by flash chromatography through a short silica column using petroleum ether as eluent.

Colourless oil, yield: 81 %. Anal. calc. for C_5H_9NS (%): C, 52.13; H, 7.87; N, 12.16; S, 27.84. Found: C, 52.56; H, 7.92; N, 27.47. FT-IR (single-bounce diamond ATR crystal, cm^{-1}): ν(CH) 2925, ν(N=C=S) 2120. ^{1}H NMR (400.13 MHz, $CDCl_3$): 3.28-3.29 (d, 2H, J = 6.29 Hz, CH), 1.89-1.98 (m, 1H, CH), 0.95 (s, 3H, CH_3), 0.94 (s, 3H, CH_3). ^{13}C NMR (100.61 MHz, $CDCl_3$): 129.4, 52.3, 29.6, 19.7.

2.2.2 Typical procedure for the preparation of di- and trisubstituted thioureas.

To a solution of isothiocyanate (0.05 mol) in dry toluene (75 ml), amine (0.052 mol) was added in one portion with permanent stirring at room temperature. The reaction was stirred for several hours under the monitoring by TLC. After the reaction mixture was passed through a short silica gel column, the solvent was removed on a rotary evaporator under reduced pressure to give corresponding thiourea. The product was used without further purification.

(Z)-N-(octadec-9-enyl)-N′-phenylthiourea (**TU 1**)

White semisolid, yield: 96 %. Anal. calc. for $C_{25}H_{42}N_2S$ (%): C, 74.57; H, 10.51; N, 6.96. Found: C, 74.61; H, 10.56; N, 6.89. FT-IR (single-bounce diamond ATR crystal, cm^{-1}): ν(NH) 3232, ν(CH) 2919, ν(Ar) 1668, ν(C=S) 1246. ^{1}H NMR (400.13 MHz, $CDCl_3$): 8.52 (s, 1H, NH), 7.40 (t, *J* = 7.86 Hz, 2H, Ar), 7.20 – 7.28 (m, 3H, Ar), 6.07 (s, 1H, NH), 5.31 – 5.37 (m, 2H, CH=CH), 3.56 -3.61 (m, 2H, NH-CH_2), 1.95 - 2.02 (m, 4H, CH_2, CH_2), 1.50 – 1.57 (m, 2H, CH_2), 1.23 – 1.33 (m, 22H, 11CH_2), 0.86 (t, *J* = 6.74 Hz, 3H, CH_3). ^{13}C NMR (100.61 MHz, $CDCl_3$): 180.3, 136.5, 129.1, 128.3, 127.1, 125.2, 45.5, 29.8, 29.6, 29.4, 29.0, 27.3, 26.9, 22.8, 14.2.

N-phenylmorpholine-4-carbothioamide (**TU 2**)

White solid, yield: 94 %. Anal. calc. for $C_{11}H_{14}N_2OS$ (%): C, 59.43; H, 6.35; N, 12.60; S, 14.42. Found: C, 60.01; H, 6.48; N, 12.54; S, 14.31. FT-IR (single-bounce diamond ATR crystal, cm^{-1}): ν(NH) 3230, ν(CH) 2915, ν(Ar) 1661, ν(N=C=S) 2121. ^{1}H NMR (400.13 MHz, $CDCl_3$): 7.52 (s, 1H, NH), 7.32 (t, 2H, *J* = 7.8 Hz, Ar), 7.15 (t, 1H, *J* = 7.4 Hz, Ar), 7.11 – 7.13 (d, 2H *J* = 7.77, Ar), 3.76 – 3.78 (m, 4H, CH_2-O-CH_2), 3.67 – 3.69 (m, 4H, CH_2-N-CH_2). ^{13}C NMR (100.61 MHz, $CDCl_3$): 183.6, 140.0, 129.3, 125.5, 123.4, 66.2, 49.7.

N-allyl-N′-phenylthiourea (**TU 3**)

White solid, yield: 98 %. Anal. calc. for $C_{10}H_{12}N_2S$ (%): C, 62.46; H, 6.29; N, 14.57; S, 16.68. Found: C, 62.59; H, 6.33; N, 14.47; S, 16.52. FT-IR (single-bounce diamond ATR crystal, cm^{-1}): ν(NH) 3227, ν(CH) 2925, ν(Ar) 1672, ν(N=C=S) 2127. ^{1}H NMR (400.13 MHz, $CDCl_3$): 8.13 (s, 1H, NH), 7.43 (t, 2H, *J* = 7.72 Hz, Ar), 7.31 (t, 1H, *J* = 7.4 Hz, Ar), 7.24 – 7.22 (d, 2H, *J* = 7.5 Hz, Ar), 6.07 (s, 1H, NH), 5.91 - 5.83 (m, 1H, CH=CH_2), 5.18 – 5.13 (m, 2H, CH=CH_2), 4.28 (t, 2H, *J* = 5.47 Hz, CH_2). ^{13}C NMR (100.61 MHz, $CDCl_3$): 180.9, 136.1, 133.4, 130.4, 127.6, 125.6, 117.3, 48.0.

N,N′-diphenylthiourea (**TU 4**)

White solid, yield: 89 %. Anal. calc. for $C_{13}H_{12}N_2S$ (%): C, 68.39; H, 5.30; N, 12.27; S, 14.04. Found: C, 68.48; H, 5.42; N, 12.13; S, 13.94. FT-IR (single-bounce diamond ATR crystal, cm^{-1}): ν(NH) 3224, ν(CH) 2926, ν(Ar) 1673, ν(N=C=S) 2130. ^{1}H NMR (400.13 MHz, $CDCl_3$): 8.00 (s, 2H, 2NH), 7.23 – 7.29 (m, 8H, Ar), 7.12 -7.16 (m, 2H Ar). ^{13}C NMR (100.61 MHz, $CDCl_3$): 179.9, 137.3, 129.7, 127.2, 125.4.

N,N′-diisobutylthiourea (**TU 5**)

White solid, yield: 96 %. Anal. calc. for $C_9H_{20}N_2S$ (%): C, 57.40; H, 10.70; N, 14.87; S, 17.03. Found: C, 57.68; H, 10.82; N, 14.67; S, 16.95. FT-IR (single-bounce diamond ATR crystal, cm_{-1}): ν(NH) 3221, ν(CH) 2924, ν(N=C=S) 2125. ^{1}H NMR (400.13 MHz, $CDCl_3$): 5.88 (s, 2H, 2NH), 3.24 (s, 4H, 2CH_2), 1.86-1.94 (m, 2H, 2CH), 0.97 (s, 6H, 2CH_3). ^{13}C NMR (100.61 MHz, $CDCl_3$): 181.9, 52.0, 28.3, 20.4.

2.3 Synthesis of QDs

2.3.1 Synthesis of Cd and Zn precursors.

Zinc oxide (ZnO, 0.0028 mol, 0.23 g), cadmium oxide (CdO, 0.0005 mol, 0.064 g), linoleic acid (LA, 0.01 mol, 2.80 g) and 1-octadecene (ODE, 4 ml) were placed in a three-necked flask equipped with a magnetic stirrer, thermometer and a reflux condenser. The reaction mixture was degassed for 20 minutes at room temperature and then for 20 minutes at 100 °C. Onwards it was heated up to 260 °C under an argon flow with vigorous stirring until complete homogenization indicated the formation of cadmium and zinc linoleates. The temperature growth rate is the same for all performed syntheses.

2.3.2 Synthesis of QDs: Hot-injection method.

A solution of thiourea **TU 1** (0.0033 mol) and oleylamine (OAm, 0.005 mol) in 1 ml ODE, freshly prepared before synthesis at 50 – 60 °C in argon atmosphere, was added in one portion to the resulting linoleates mixture at the certain temperature (220 – 300 °C). At the moment of precursor's injection, the temperature of the reaction mixture sharply dropped by 10 °C and stabilized after 6 minutes. The growth of QDs continued for 30 minutes, after which the reaction mixture was cooled to 50 °C and transferred into $CHCl_3$ for purification. The growth of nanocrystals was monitored by taking aliquots from the reaction mixture from the moment of the precursor's injection until the reaction mixture was cooled. The aliquots (35 μl) were dissolved in 2 ml of $CHCl_3$ for further measurements of the absorbance and photoluminescence spectra.

2.3.3 Synthesis of QDs: One-pot method.

The mixture of Cd and Zn linoleates mentioned above was cooled to 50 °C. A freshly prepared solution of substituted thiourea (**TU 1 - 5**) (0.0033 mol), OAm (0.005 mol) in 1 ml of ODE was added to the mixture of linoleates with stirring in Ar atmosphere. Later on, the temperature of the reaction mixture was evenly raised to a certain temperature (220 – 300 °C). Starting from 170 °C, aliquots were taken systematically and further were dissolved in $CHCl_3$ for optical properties measurements. The growth of QDs lasted for 30 minutes. Onwards, the mixture was cooled to 50 °C for isolation and purification of QDs.

2.3.4 Isolation and purification of nanocrystals.

The reaction mixture was cooled to 50 °C and then was transferred into 25 ml of $CHCl_3$. Acetone was added to this solution in small portions with stirring until a stable suspension was formed. The separation of QDs was performed by centrifugation at 10,000 rpm for 7 minutes. The separated particles were further re-dissolved in $CHCl_3$ and then precipitated by acetone to remove the reaction by-products and solvent. This procedure was repeated for three times. After purification and separation, the precipitate was dried in vacuum for 5 hours at room temperature.

2.4 Characterization

The Nuclear Magnetic Resonance (NMR) spectra were recorded from solutions in $CDCl_3$ at 295 K on a Bruker 400 UltraShield^{TM} spectrometer (equipped with a Z-gradient 5 mm BBO probe at frequencies 400.13 MHz for ^{1}H and 100.61 MHz for ^{13}C $\{^{1}H\}$). The solutions were obtained by dissolving approximately 50 mg of each compound in 0.6 ml of $CDCl_3$. The values of ^{1}H chemical shifts were calibrated to residual signals of $CDCl_3$ (δ (^{1}H) = 7.26 ppm).

The values of ^{13}C chemical shifts are referred to signals of $CDCl_3$ (δ (^{13}C) = 77.23 ppm). Positive chemical shift values denote shifts to the higher frequencies relative to the standards.

IR spectra in the region 4000 – 400 cm^{-1} (resolution 2 cm^{-1}) were recorded on Vertex 70v FTIR spectrometer (Bruker, Germany) using single-bounce diamond ATR crystal. X-Ray diffraction patterns (XRD) were registered using PANalytical EMPYREAN powder X-ray diffractometer (ALMELO, Netherlands) with Cu-K_α radiation (λ = 1.5418 Å). Data were obtained across a 2θ range of 20 – 70° with a step size of 0.05°.

Transmission electron microscopy (TEM) measurements were performed with state-of-the-art TEM FEI TITAN Themis 60-300 Cubed operated at 300 keV. To visualize the QDs with a diameter around few nanometers, high resolution (HR)-TEM and scanning TEM (HR-STEM) techniques were used. Energy dispersive X-ray (EDX) spectroscopy was performed to analyze the chemical composition of QDs. The analysis was done in STEM mode (STEM-EDX) with FEI SUPER-X 4-quadrant windowless detector with 120 mm^2 total detection area and 0.7 sr solid angle.

The thermal decompositions of $Cd_{0.15}Zn_{0.85}S$ QDs were investigated using a thermogravimetric analyzer (Pyris 1 TGA, PerkinElmer, USA) coupled to gas-chromatography mass spectrometer (GC Clarus 680, MS Clarus SQ 8T, PerkinElmer, USA). Samples (about 25 mg) were heated from room temperature to 650 °C at a heating rate of 40 °C/min under flowing N_2 (20 ml/min; Linde). The precision of temperature measurement was 5 °C. TGA furnace chamber outlet was connected to the GC/MS instrument through a hot capillary column (TL 8500) heated to 280 °C. The GC/MS conditions were as follows: capillary chromatographic column Elite-5MS (30 mm × 0.25 mm × 0.25 μm); EI (70 eV); full scan (5 – 450 m/z). Data analysis was performed using TurboMass™ GC/MS Software.

The QDs optical properties were measured using Fluorometer PTI QuantaMaster 400 (Horiba, Germany) to obtain PL data in spectral range 300 – 700 nm using excitation wavelength λ = 300 – 400 nm and UV-3600 (Shimadzu, Japan) spectrometer to get UV-VIS absorbance spectra in the spectral range 200 – 700 nm.

3. Results and discussion

3.1 Synthesis of sulfur precursors

Figure 1 presents a general scheme for the synthesis of N,N′-disubstituted and N,N′,N′-trisubstituted thioureas, which were used for the preparation of $Cd_{0.15}Zn_{0.85}S$ QDs. This synthesis was carried out at room temperature according to the technique described earlier [20].

Phenyl- and allyl isothiocyanates were purchased from Sigma-Aldrich and used without further modifications. *i*-Butyl isothiocyanate was synthesized according to the presented scheme (Figure 1) and the reaction was carried out in the presence of a catalyst (2,4,6-trichloro-1,3,5-triazine (TCT)) through the formation of intermediate potassium *i*-butyl dithiocarbamate [21]. All synthesized species were isolated, purified and characterized by NMR and IR spectroscopy.

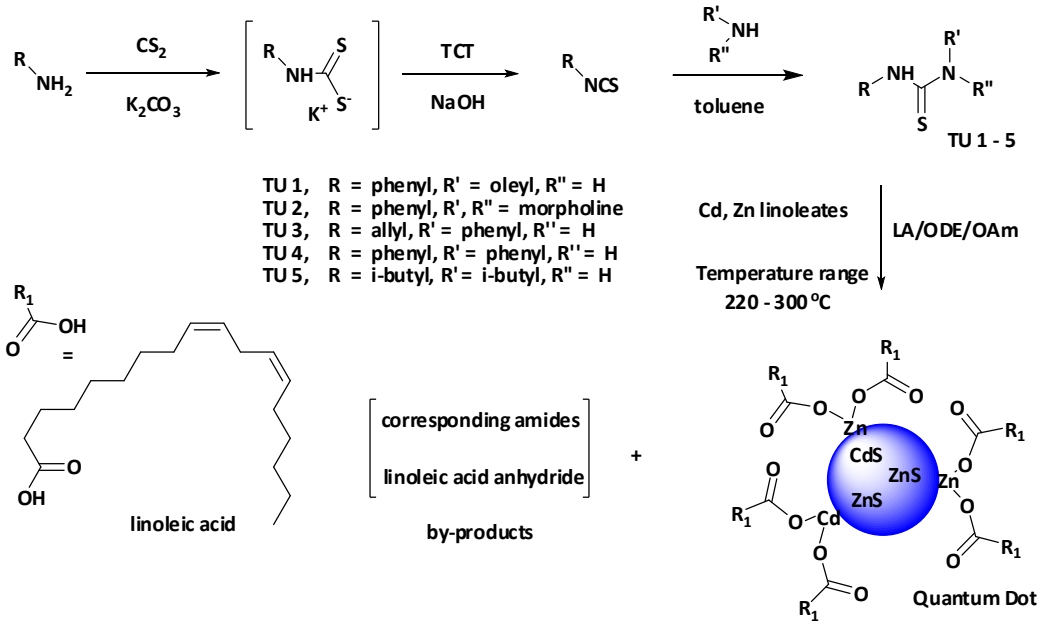

Figure 1. The general synthesis scheme of $Cd_{0.15}Zn_{0.85}S$ Quantum Dots.

3.2 Synthesis of $Cd_{0.15}Zn_{0.85}S$ QDs quantum dots

All syntheses of $Cd_{0.15}Zn_{0.85}S$ QDs were conducted in a three-necked flask under an argon atmosphere. The temperature of the reaction medium was maintained by external heating in a Wood's metal bath. Homogeneity of the heating and distribution of the components was achieved by using a magnetic stirrer in the reaction mixture. The N,N′- disubstituted (or N,N′,N′-trisubstituted) thiourea was dissolved in a mixture of OAm and ODE with slight heating (about 50 °C) and then this mixture was injected into a solution of cadmium and zinc linoleates through a self-sealing membrane.

During the dissolving of substituted thiourea in OAm, the temperature control should be accurate due to the fast exchange reaction between substituents in thiourea and oleylamine with a formation of substituted oleylthiourea. In the case of synthesis by a hot-injection method, the sulfur precursor solution was injected to the reaction medium at a chosen temperature for certain synthesis. In contrast, in a one-pot method, the sulfur precursor solution was added to the reaction mixture at 50 °C. After that, the temperature was raised at the same speed for all syntheses up to the selected temperature for QDs growth. To maintain a constant volume of the solution, a reflux system was used. To avoid oxidation of the reagents, all syntheses were carried out under an argon atmosphere.

3.3 Mechanism of nanocrystal's formation

In order to investigate the kinetics of nucleation and growth of nanocrystals, a two-way study was performed. The one-pot and the hot-injection synthetic methods were conducted in parallel keeping the same ratios of all components and their concentrations in the reaction medium, at the temperature range from 220 °C till 300 °C with 20 °C step. It should be remarked that the most significant influence of temperature was observed for $Cd_{0.15}Zn_{0.85}S$ QDs obtained by the hot-injection method. At the same time, $Cd_{0.15}Zn_{0.85}S$ QDs obtained by the one-pot method revealed no significant differences between their structural characteristics and optical properties. We assume that during the reaction of metals' linoleates and N,N′-

disubstituted thiourea, the temperature has the greatest influence on the decomposition process of formed complexes and, hence, on nucleation, whereas further growth of QDs is not so strongly affected by temperature. Thus, at the moment of the sulfur precursor injection ("instantaneous nucleation" - hot-injection method) or attaining of a suitable temperature ("time-consuming nucleation" - one-pot method), nucleation occurs and the reaction medium instantaneously reaches the saturation. After that, the nuclei grow further by taking up free precursors of metals and sulfur from the reaction mixture. From saturated solution nuclei, growth occurs quite rapidly, which can be monitored by changes in the absorbance spectra. After the solution reached saturation by growing of nuclei, a phenomenon called Ostwald ripening may occur (particles, which have reached a critical size, grow at the expense of dissolution of the smaller particles). Thereby, there is a tendency to reduce the surface free energy of the system, which is provided by the smallest crystals. Following the tendency to grow and decreasing the solution's saturation, at each instant the critical size of the crystal is changing in the system.

Simultaneous nucleation, in which nuclei are created at the same moment and further experiencing the same growth conditions, ensures the uniformity of the nanocrystals. The particle size is controlled by taking aliquots at different time intervals from the reaction mixture, which makes possible to estimate the sample properties by the position of the PL_{max} (Figure 2a, 2c) and first exciton maximum in the photoluminescence and absorbance spectra respectively (Figure 2b, 2d).

It should be noted that during the synthesis by one-pot method nanocrystals' formation occurs at the fairly low temperature and the first exciton maximum in the absorbance spectrum shows up at 170 °C (Figure 2b). In the case of the synthesis by hot-injection method, this maximum appears right after the injection of N,N′-disubstituted thiourea (Figure 2d). Such fast growth induced by the high reactivity of N,N′-disubstituted thiourea and the rate of its decomposition is also monitored in the absorbance and photoluminescence spectra.

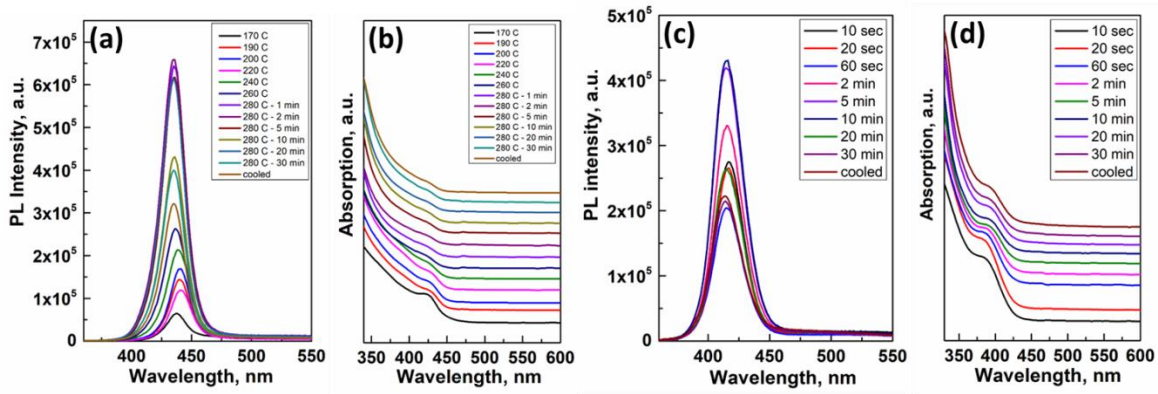

Figure 2. Photoluminescence and UV-Vis absorbance spectra of $Cd_{0.15}Zn_{0.85}S$ QDs prepared by one-pot (a, b) and hot-injection (c, d) methods with **TU 1** at 280 °C.

3.4 Structural analysis and morphology of $Cd_{0.15}Zn_{0.85}S$ QDs

Figure 3a, b represents XRD patterns of $Cd_{0.15}Zn_{0.85}S$ QDs synthesized by one-pot and hot-injection methods in a range of temperatures from 220 to 300 °C. All compounds possessed a similar crystal structure. In accordance with the experimental data, QDs crystallized in a face

centred cubic phase with the space group F-43*m*. Three broad diffraction peaks were observed at 2θ = 28.1, 46.4 and 55.2 indicating (111), (220) and (311) planes respectively.

The first peak has the highest intensity indicating that the preferred orientation in the crystal occurs along the (111) crystal plane. No additional diffraction peaks of CdO, ZnO or other impurities were observed. As one can see in Figure 3b, the size of QDs obtained by hot-injection method is increasing with an increase of temperature.

The lattice parameters *a* of $Cd_{0.15}Zn_{0.85}S$ QDs were calculated according to standard equation (1) for a cubic crystal system [22]:

$$\frac{1}{d^2} = \frac{h^2+k^2+l^2}{a^2} \quad (1)$$

where *h*, *k* and *l* are Miller indices, *d* is the interplanar distance and *a* is the lattice parameter. Calculated lattice parameters are summarized in Table 1.

The average crystal size was calculated according to the Debye Scherrer's equation [23]:

$$d = \frac{K\lambda}{\beta \cos\theta} \quad (2)$$

where *d* is the particle size, λ is the X-ray wavelength, and β is the full width at half maximum (FWHM) of the diffraction peak at 2θ (θ is the Bragg diffraction angle). The average crystalline sizes are listed in Table 1. The mean crystalline size of $Cd_{0.15}Zn_{0.85}S$ nanocrystals is in the range of 3 – 4 nm. Thus, the obtained results for all prepared QDs are in a good agreement with previously published results [22, 24].

As described above, $Cd_{0.15}Zn_{0.85}S$ QDs prepared with (Z)-N-(octadec-9-enyl)-N′-phenylthiourea formed a single phase with cubic zinc blende structure with the space group F-43*m* (Figure 3c). It matches well with the standard for ZnS found in the database (JCPDS No. 66-0174). It can be clearly seen that despite the use of various thioureas, the crystal structure of $Cd_{0.15}Zn_{0.85}S$ QDs remains unchanged. The crystalline size was found to be dependent on the chain length of the organic ligands. The smallest quantum dots (2.9 nm) were obtained on the N,N′-diisobutylthiourea, the biggest one (4.6 nm) – on the (Z)-N-(octadec-9-enyl)- N′-phenylthiourea (Table 1).

Table 1. Structural parameters of $Cd_{0.15}Zn_{0.85}S$ QDs.

Method	Lattice parameter *a*, Å	Space group	Mean crystalline size, nm
One pot:			
220 °C	5.4939 (2)	F-43*m*	3.2
240 °C	5.4838 (1)	F-43*m*	4.1
260 °C	5.4753 (1)	F-43*m*	4.6
280 °C	5.4772 (5)	F-43*m*	4.6
300 °C	5.4943 (9)	F-43*m*	4.2
Hot-injection:			
220 °C	5.4915 (6)	F-43*m*	3.1
240 °C	5.5141 (7)	F-43*m*	3.3
260 °C	5.5304 (4)	F-43*m*	3.8
280 °C	5.4829 (1)	F-43*m*	3.9
300 °C	5.5006 (1)	F-43*m*	4.2
One pot with different thioureas:			
TU 1	5.4753 (1)	F-43*m*	4.6
TU 2	5.4781 (1)	F-43*m*	3.9
TU 3	5.4659 (8)	F-43*m*	3.5
TU 4	5.4884 (6)	F-43*m*	3.7
TU 5	5.4906 (4)	F-43*m*	2.9

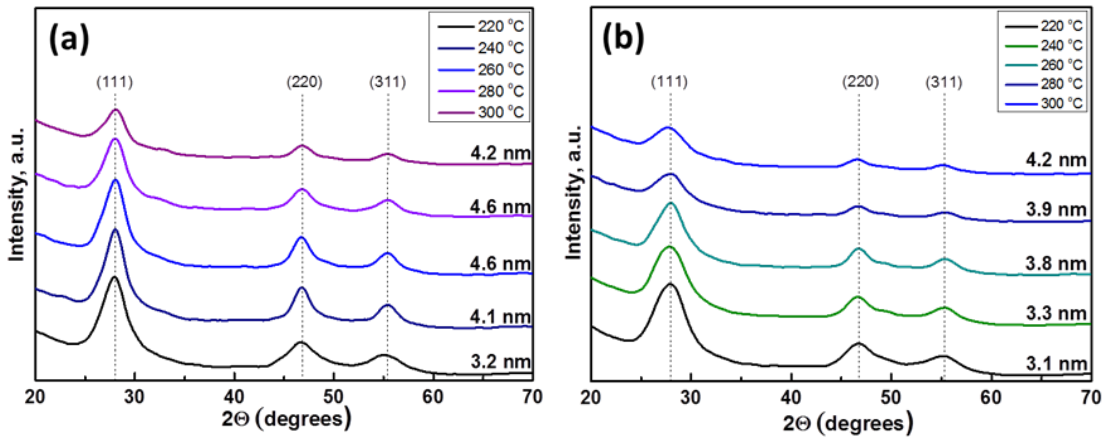

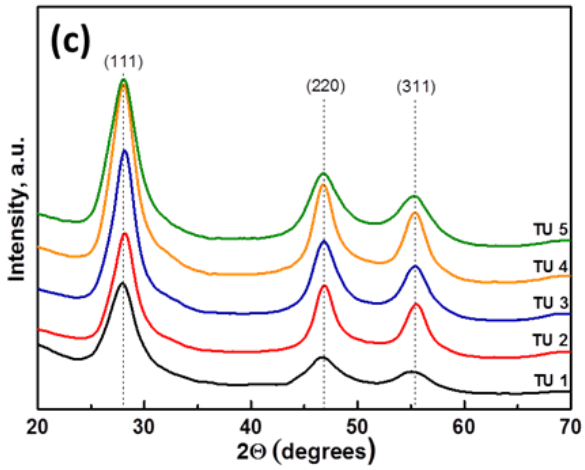

Figure 3. XRD pattern of $Cd_{0.15}Zn_{0.85}S$ QDs a) synthesized by one-pot method at different temperatures (QDs size from 3.2 nm to 4.6 nm); b) synthesized by hot-injection method at different temperatures (QDs size from 3.1 nm to 4.2 nm); c) synthesized by one-pot method at 260 °C with thioureas **TU 1 – 5.**

Figure 4 demonstrates TEM images for as-prepared $Cd_{0.15}Zn_{0.85}S$ QDs. The provided solutions of QDs in hexane were sonicated for few minutes and instantly dropped on a transmission electron microscopy (TEM) copper grid with electron transparent membrane from amorphous carbon. From Figure 4 it can be seen that nanoparticles are quite monodisperse and have nearly spherical shape except for one (Figure 4f) prepared with N,N′-diisobutylthiourea. These nanoparticles have the shape of a parallelogram.

HAADF STEM imaging and corresponding energy dispersive X-ray spectroscopy (EDS) mapping presented in Figure 5a–d. These results reveal that Cd, Zn and S are distributed homogeneously in QDs. There is no apparent element aggregation or separation. Also, the carbon and oxygen signals were confirmed in EDS spectra and correspond to their content in the organic shell. The nitrogen signal was also found in EDS and can be attributed to traces of the oleylamine, which is present in organic shell as an additional ligand. The intensity of these signals is in a good agreement with nominal compositions of QDs.

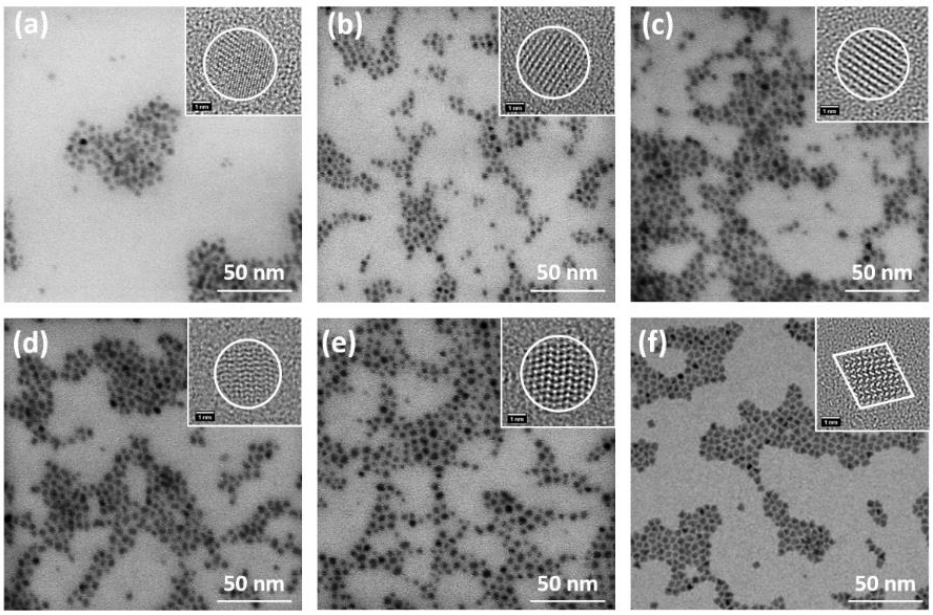

Figure 4. TEM images of $Cd_{0.15}Zn_{0.85}S$ QDs (with a high-magnification TEM image shown in the inset) prepared at 260 °C by (a) one-pot method with **TU 1**, (b) hot-injection method with **TU 1**, (c) one-pot method with **TU 2**, (d) one-pot method with **TU 3**, (e) one-pot method with **TU 4**, (f) one-pot method with **TU 5**.

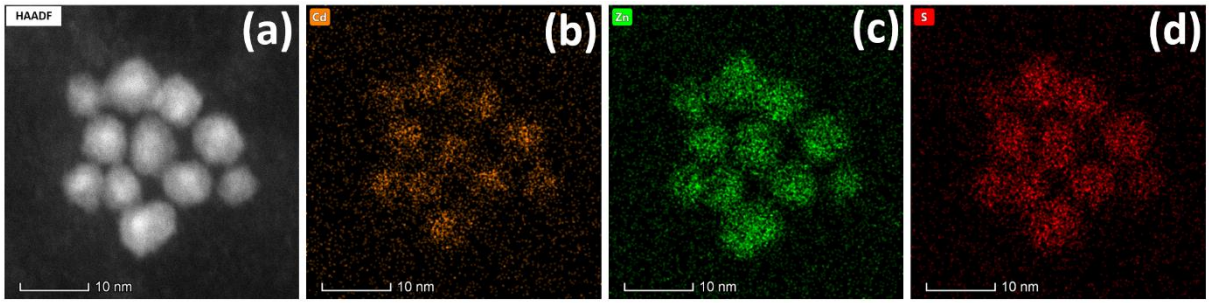

Figure 5. (a) HAADF-STEM image; corresponding EDS elemental mapping: (b) Cd elemental map (orange); (c) Zn elemental map (green); (d) S elemental map (red) of $Cd_{0.15}Zn_{0.85}S$ QDs prepared at 260 °C by one-pot method with **TU 1**.

Table 2 summarizes results of the elemental analysis of $Cd_{0.15}Zn_{0.85}S$ QDs conducted by EDS. It was found that the measured Cd : Zn ratio is very close to the ratios of the starting materials taken to the reaction (0.15 : 0.85) for all experiments. We assume that reactivity of Zn and Cd cations with substituted thioureas is comparable in the entire temperature range. Thus, based on data mentioned above, *i.e.* comparing the size of QDs and cation's reactivity, we suppose that the synthesized QDs have a homogeneous structure. Only minor influence of the substituents' nature in substituted thioureas on the cations ratio was noticed. It was confirmed that CdZnS nanocrystal as a structural unit represents a hybrid cadmium-zinc sulfide, enclosed in a protective organic shell. Such shell consists of the carboxylates of the same metals [25, 26]. Due to that, metal : sulfur ratio in discussed compositions is not stoichiometric and strongly depends on the QDs size.

Table 2. Elemental composition of $Cd_{0.15}Zn_{0.85}S$ QDs measured by EDS.

Method	Cd, at.%	Zn, at.%	S, at.%	Cd : Zn ratio
One pot:				
220 °C	9.41	50.52	40.07	14.6 : 85.4
240 °C	8.84	50.02	41.14	14.8 : 85.2
260 °C	9.01	50.01	40.98	14.9 : 85.1
280 °C	8.62	51.67	39.71	14.4 : 85.6
300 °C	9.14	51.19	39.67	14.6 : 85.4
Hot-injection:				
220 °C	9.26	52.71	38.03	14.6 : 85.4
240 °C	9.14	52.19	38.67	14.8 : 85.2
260 °C	9.34	50.55	40.11	15.8 : 84.2
280 °C	8.85	50.36	40.79	14.1 : 85.9
300 °C	9.71	50.37	39.92	14.7 : 85.3
One pot with different thioureas:				
TU 1	9.01	50.01	40.98	14.9 : 85.1
TU 2	9.32	50.34	40.34	15.1 : 84.9
TU 3	8.82	52.72	38.45	14.5 : 85.5
TU 4	9.74	49.02	41.24	15.9 : 84.1
TU 5	9.49	49.84	40.67	16.0 : 84.0

3.5 Thermogravimetric study of $Cd_{0.15}Zn_{0.85}S$ QDs

The thermal stability was examined by thermogravimetric analysis (TG). The thermogravimetric and derivative thermogravimetric (DTG) curves of $Cd_{0.15}Zn_{0.85}S$ QDs prepared by one-pot method and hot-injection method are shown in Figure 6a and 6b, respectively. All experiments were performed under identical experimental conditions for a heating rate of 40 °C/min.

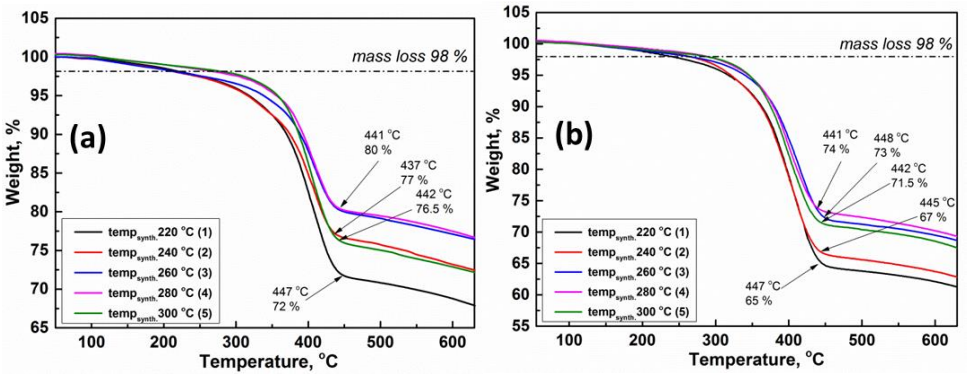

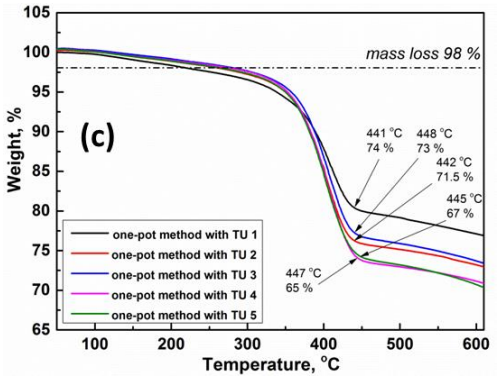

Figure 6. TG analysis of $Cd_{0.15}Zn_{0.85}S$ QDs prepared at 260 °C by (a) one-pot method with **TU 1**, (b) hot-injection method with **TU 1** (c) one-pot method with **TU 1 - 5**.

All the TGA curves have a similar trend and the thermal degradation of samples occurs in the temperature range of 220 to 450 °C (the exact values of temperature for each sample are shown in Table 3) which is due to the loss of organic compounds used during the synthesis of QDs. A linear dependence with the slope about 0.11 %(°C)$^{-1}$ and 0.16 %(°C)$^{-1}$ is observed for one-pot method and hot-injection method, respectively. From the shape of TGA curves, it seems that the thermal degradation takes place in the one-step process, however, two noticeable maxima of DTG curve can be detected. The first one at 312 – 340 °C, corresponds to oleylamine (as an additional ligand in the organic shell of QDs). The second peak, at 400 – 413 °C, corresponds to the anion of metal carboxylates (*i.e.* linoleic acid). Values of both DTG maxima are summarized in Table 3.

From the decomposition temperature range summarized in Table 3, the information on the thermal stability of QDs prepared by the different method can be obtained. It is evident that the value of residue and $T_{98wt\%}$ increase with preparation temperature.

As mentioned above, in the same way, the size of QDs is influenced by the reaction conditions. From the comparison of these results, it can be concluded that the size of QDs influences their thermal stability, which is particularly evident on QDs prepared by hot-injection method. This is consistent with the results presented by Wageh and co-workers [27].

Figure 6c shows TG curves of $Cd_{0.15}Zn_{0.85}S$ QDs synthesized with different substituted thioureas. The temperature range of decomposition, temperatures of DTG peaks and value of residue are summarized in Table 3. The lowest mass loss (22.9 %) was detected for the biggest quantum dots (4.6 nm) synthesized with **TU 1**. On the contrary, the highest mass loss (29.3 %) was found for the smallest quantum dots (2.9 nm), which were synthesized with **TU 5**. The TG/DTG thermograms for all synthesized $Cd_{0.15}Zn_{0.85}S$ QDs are presented in *Supplementary Materials Fig. S1 - 3.*

Table 3. Results from TG/DTG curves of $Cd_{0.15}Zn_{0.85}S$ QDs. Mass loss comparison measured by thermal decomposition.

Method	Decomposition range ($T_{98wt\%}$ - T_{end}), °C	Residue at T_{end}, %	1st DTG peak, °C	2nd DTG peak, °C	Residue at 600 °C, %
One pot:					
220 °C	226 – 448	72	322	404	68.8
240 °C	219 – 439	77	325	406	73.2
260 °C	221 – 437	80	337	411	77.1
280 °C	276 – 440	80	340	406	77.5
300 °C	288 – 440	76	338	404	72.9
Hot-injection:					
220 °C	239 – 445	65	316	402	62.1
240 °C	262 – 442	67	312	407	63.7
260 °C	262 – 448	72	323	413	69.5
280 °C	287 – 439	74	312	401	70.2
300 °C	285 – 442	71.5	–	400	68.5
One pot with different thioureas:					
TU 1	221 – 437	80	337	411	77.1
TU 2	263 – 436	76	-	403	73.2
TU 3	284 – 439	77	-	407	73.7
TU 4	279 – 441	74	-	405	71.2
TU 5	266 – 443	75	-	400	70.7

3.6 FT-IR spectral studies of $Cd_{0.15}Zn_{0.85}S$ QDs

The Fourier Transform Infrared Spectroscopy (FT-IR) was used for the identification of the organic ligand in synthesized nanopowders. Measurements were conducted in the range of 4000 – 400 cm^{-1} at room temperature. The FT-IR spectrum of QDs prepared by one-pot method at 260 °C (blue line) compared with the linoleic acid (black line) and oleylamine (red line) is given in Figure 7. FT-IR spectra of QDs prepared by other methods are shown in *Supplementary materials Fig. S4*.

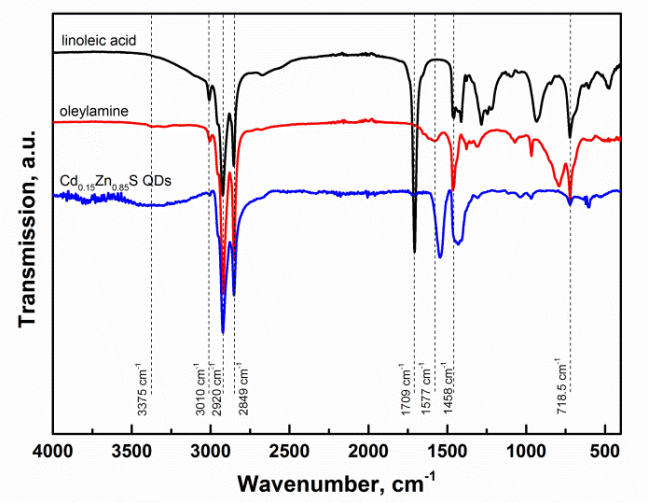

Figure 7. FT-IR spectra of prepared $Cd_{0.15}Zn_{0.85}S$ QDs (blue line) in comparison with linoleic acid (black line) and oleylamine (red line).

The broad band appearing in the region of 3500 – 3100 cm^{-1} corresponds to the stretching vibrations of the O-H group, which indicates the presence of solvating water molecules [28]. In the same region, weak peaks at 3298 and 3375 cm^{-1} were assigned to NH_2 stretching vibrations in the oleylamine molecule, which are associated with symmetric and asymmetric modes, respectively [29]. The region 3050 – 2800 cm^{-1} is associated with the presence of hydrocarbon fragments in the molecule, in particular, the symmetric and asymmetric stretching vibrations of CH_2 and CH_3 groups. The signal at 3010 cm^{-1} represents the CH=CH-CH_2 group vibrations which exist in each demonstrated compound.

The presence of a signal in the spectrum of linoleic acid at 1709 cm^{-1} (C=O group) and its absence in the spectrum of QDs confirms the assumption that there is no free carboxyl group in the structure of QDs. The appearance of a signal at 1540 cm^{-1} in the spectrum of QDs indicates the presence of the carboxyl moiety in the form of cadmium and zinc carboxylates [30]. Also, the small shift of the C-H signal of the group from 1458 cm^{-1} to the broadened signal at 1430 cm^{-1} is observed in the spectrum of QDs. The signal at 718.5 cm^{-1}, which is visible in all structures with different intensities, confirms the presence of a double cis-bond in the molecules. Formation of Zn-S and Cd-S bonds is evidenced by the signals in the region 700 – 400 cm^{-1}, which are related to metal-sulfur bonds [31].

3.7 Optical properties of $Cd_{0.15}Zn_{0.85}S$ QDs

We have studied two approaches to the synthesis in organic disperse medium to investigate the effect of temperature on nucleation and growth of $Cd_{0.15}Zn_{0.85}S$ QDs in detail. In one-pot method, QDs' growth was monitored from 170 °C to the selected growth temperature with an interval of 10 °C by taking aliquots (35 µl), which were further dissolved in $CHCl_3$ (2 ml).

Figure 8a shows the growth of QDs as the maximum emission value (PL_{max}) dependence on time for the synthesis made by one-pot method at different temperatures. As can be seen in this figure, the changes that occur in the emission values (after the selected temperature is reached) are within the experimental error. It was confirmed that the interaction of cadmium and zinc carboxylates with substituted thioureas at relatively low temperatures (up to 100 °C) leads to the formation of a stable complex [32] which is subsequently decomposed to the corresponding sulfides. This finding confirms that the temperature of synthesis has a significant influence on nucleation and slightly affects the crystal's growth.

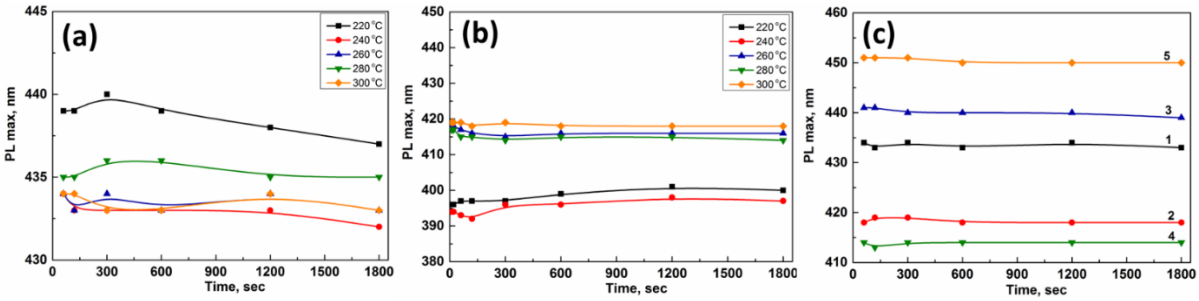

Figure 8. Summary of PL peak position at different reaction times by (a) one-pot method with **TU 1**, (b) hot-injection method with **TU 1** (c) one-pot method with **TU 1 - 5**.

Figure 8b presents the effect of the temperature on nucleation as a PL_{max} dependence on time for the reaction done by hot-injection method. The data reveal that with raising the temperature, the red shift of PL maximum occurs (from 396 to 417 nm) and these values correlate favorably with the QDs sizes. Moreover, significant changes in the PL_{max} position (from 413 to 450 nm) with the replacement of substituents in thioureas were observed (Figure 8c). We suppose that these changes can be explained by the different stability of substituted thioureas and their complexes with cadmium and zinc carboxylates. It should be noted that with the use of substituted thiourea as a sulfur source in the synthesis of Cd-Zn-S QDs, the reaction proceeds rapidly to achieve full conversion. That fact ensures the production of highly photoluminescent QDs. The uniformity of crystals in size and shape can be clearly seen from the FWHM values presented in Table 4. For all obtained QDs the FWHM values vary in a narrow range from 23 to 32 nm.

Table 4 summarizes the relative photoluminescence quantum yield (PL QY) values for the isolated and purified $Cd_{0.15}Zn_{0.85}S$ QDs. The calculation of PL QY was carried out according to the formula:

$$PL\ QY_{QD} = PL\ QY_{ref} \frac{PL_{QD}}{PL_{ref}} \frac{ABS_{ref}}{ABS_{QD}} \frac{n_{CHCl_3}}{n_{ethanol}} \quad (3)$$

where PL QY_{QD} is the PL quantum yield of synthesized QDs, PL QY_{ref} is the PL quantum yield of Coumarin 334 as a reference (PL QY_{ref} = 0.69) [33], ABS_{QD} and ABS_{ref} are optical densities at the excitation wavelength (375 nm) and the refractive indices (n) of the solvents.

Table 4. Optical properties of $Cd_{0.15}Zn_{0.85}S$ QDs. Peak maximum of the emission in photoluminescence spectra (λ_{PL}), peak maximum of the first transition in the absorbance spectra (λ_{ABS}), Stokes shift, FWHM, bandgap energy E_g and relative photoluminescence quantum yield (PL QY).

Method	λ_{PL}, nm	λ_{ABS}, nm	Stokes shift, nm	FWHM, nm	E_g, eV	PL QY, %
One pot:						
220 °C	437	425	12	26	3.52	48
240 °C	431	420	11	26	3.43	61
260 °C	433	422	11	25	3.52	67
280 °C	435	426	9	23	3.50	48
300 °C	434	425	9	26	3.47	58
Hot-injection:						
220 °C	400	393	7	28	3.37	51
240 °C	396	380	16	25	3.42	56
260 °C	416	398	18	32	3.44	59
280 °C	415	394	21	29	3.41	58
300 °C	417	395	22	30	3.44	65
One pot with different thioureas:						
TU 1	433	422	11	25	3.51	67
TU 2	416	392	24	31	3.46	45
TU 3	440	430	10	26	3.41	46
TU 4	413	391	22	27	3.44	42
TU 5	450	432	18	32	3.43	43

The difference in the absorbance and emission energies, called the Stokes shift, is caused by electron relaxation. Figure 9 presents a comparison between the absorbance and photoluminescence spectra (excitation wavelength λ_{exc} = 350 nm) obtained for pure $Cd_{0.15}Zn_{0.85}S$ QDs. The measurements were carried out in $CHCl_3$ solution in the air at room temperature. The optical density of solutions was 0.1. The symmetry of the signals, their shape, and values of Stokes shift indicate the uniformity of nanocrystals in both shape and size. It is the shape and size of QDs together with their composition that determine their bandgap. Therefore, a significant advantage of ternary quantum dots over binary ones is expected. The absorbance spectra were used for estimation of optical band gaps E_g of synthesized $Cd_{0.15}Zn_{0.85}S$ QDs (*Supplementary materials Fig. S11*).

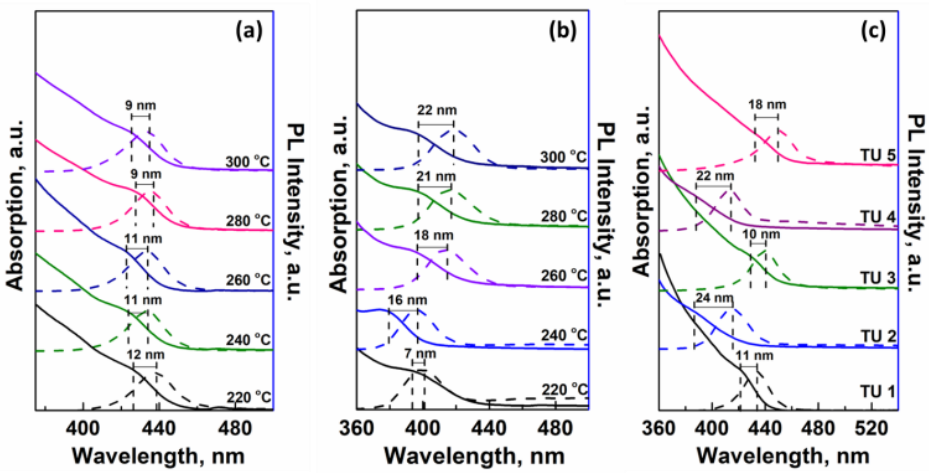

Figure 9. Stokes shift in comparison of absorbance (solid lines) and emission spectra (dashed lines) of $Cd_{0.15}Zn_{0.85}S$ QDs (a) one-pot method with **TU 1**; (b) hot-injection method with **TU 1**; (c) one-pot method at 260 °C with **TU 1 - 5**.

Considering $Cd_{0.15}Zn_{0.85}S$ to be direct band gap semiconductor we can approximate spectral dependence of absorbance coefficient close to band gap energy by Tauc relation in the form:

$$(\alpha h\nu) \sim (h\nu - E_g)^{1/2} \quad (4)$$

where $h\nu$ is incident photon energy. Consequently, band gaps values can be determined by constructing a Tauc plot as a dependence of $(\alpha h\nu)^2$ vs. $h\nu$. The E_g value is then obtained by linear extrapolation of nearly linear $(\alpha h\nu)^2$ dependence in UV part of the spectra. The intersection of this extrapolated line with $h\nu$ axis gives the value of E_g and these values are listed in Table 4. It is worth to note that determined E_g values of $Cd_{0.15}Zn_{0.85}S$ QDs correlate with corresponding E_g bulk values of CdS and ZnS binary compounds (E_g[CdS] = 2.42 eV, E_g[ZnS] = 3.61 eV) [6].

4. Conclusions

In this paper, we have presented the development of the synthetic route leading to ternary $Cd_{0.15}Zn_{0.85}S$ QDs with the use of di- and trisubstituted thioureas as a new sulfur source. Successfully applying two approaches to the synthesis in an organic dispersion medium, namely one-pot and hot-injection methods, a detailed study on the thermal mode, *i.e.* the effect of temperature on nucleation and nanocrystal growth for each method, was carried out. The adaptation of new sulfur sources to the temperature conditions was performed. The influence of substituents (aliphatic, aromatic and heterocyclic fragments) in substituted thioureas on the synthesis kinetics and optical properties of the resulting nanomaterials has been described. We have successfully replaced toxic and expensive sulfur precursors (for example, trioctyl- and tributylphosphine sulfides) with inexpensive and environmentally friendly substituted thioureas. We have obtained comprehensive results demonstrating the possibility to conduct this synthesis at lower temperatures with high conversion of the desired product. The findings of the study show that uniform and highly photoluminescent (PL

QY up to 67 %) $Cd_{0.15}Zn_{0.85}S$ QDs with an average size of 2.9 to 4.6 nm in diameter can be easily transferred to industrial production, due to the high reproducibility and safety of the presented methods.

Acknowledgements

Authors appreciate financial support from project “High-sensitive and low-density materials based on polymeric nanocomposites” – NANOMAT (№ CZ.02.1.01/0.0/0.0/17_048/0007376), support from the grants LM2015082 and ED4.100/11.0251 from the Ministry of Education, Youth and Sports of the Czech Republic and European Regional Development Fund-Project "Modernization and upgrade of the CEMNAT" (No. CZ.02.1.01/0.0/0.0/16_013/0001829). Part of the work was carried out with the support of CEITEC Nano Research Infrastructure (ID LM2015041, MEYS CR, 2016–2019), CEITEC Brno University of Technology.

References

[1] Q. Sun, Y. A. Wang, L. S. Li, D. Wang, T. Zhu, J. Xu, C. Yang, Y. Li, Bright, multicoloured light-emitting diodes based on quantum dots, Nat. Photon. 1 (12) (2007) 717-722.

[2] S. Slang, L. Loghina, K. Palka, M. Vlcek, Exposure enhanced photoluminescence of $CdS_{0.9}Se_{0.1}$ quantum dots embedded in spincoated $Ge_{25}S_{75}$ thin films, RSC Adv. 7 (2017) 53830-53838.

[3] A. Kongkanand, K. Tvrdy, K. Takechi, M. Kuno, P. V. Kamat, Quantum dot solar cells. Tuning photoresponse through size and shape control of CdSe-TiO_2 architecture, J. Am. Chem. Soc. 130 (12) (2008) 4007-4015.

[4] I. Lokteva, N. Radychev, F. Witt, H. Borchert, J. Parisi, J. Kolny-Olesiak, Surface treatment of CdSe nanoparticles for application in hybrid solar cells: the effect of multiple ligand exchange with pyridine, J. Phys. Chem. C. 114 (29) (2010) 12784-12791.

[5] J. Saha, A.D. Roy, D. Dey, D. Bhattacharjee, S.A. Hussain, Role of quantum dot in designing FRET based sensors, Mat. Tod. Proc. 5 (2018) 2306-2313.

[6] A.A.P. Mansur, H.S. Mansur, R.L. Mansur, F.G. de Carvalho, S.M. Carvalho, Bioengineered II-VI semiconductor quantum dot – carboxymethylcellulose nanoconjugates as multifunctional fluorescent nanoprobes for bioimaging live cells, Spectrochimica Acta Part A: Molec. Biomolec. Spectr. 189 (2018) 393-404.

[7] I. L. Medintz, H. T. Uyeda, E. R. Goldman, H. Mattoussi, Quantum dot bioconjugates for imaging, labelling, and sensing, Nat. Mater. 4 (6) (2005) 435-446.

[8] A.A.P. Mansur, H.S. Mansur, A.J. Caires, R.L. Mansur, L.C. Oliveira, Composition-Tunable optical Properties of $Zn_xCd_{1-x}S$ Quantum Dot – Carboxymethylcellulose conjugates: Towards One-pot Green Synthesis of Multifunctional Nanoplatforms for Biomedical and Environmental Applications, Nanoscale Res. Let. 12 (2017) 443.

[9] P. Eskandari, F. Kazemi, Z. Zand, Photocatalytic reduction of aromatic nitro compounds using CdS nanostructure under blue LED irradiation, J. Photochem. Photobiol. A. 3 (2014) 859-863.

[10] C.M. Bernt, P.T. Burks, A.W. De Martino, A.E. Pierri, E.S. Levy, D.F. Zigler, P.C. Ford, Photocatalytic carbon disulfide production via charge transfer quenching of quantum dots, J. Am. Chem. Soc. 136 (2014) 2192-2195.
[11] A. Pal, I. Ghosh, S. Sapra, B. Konig, Quantum dots in visible-light photoredox catalysis: reductive dehalogenations and C-H arylation reactions using aryl bromides, Chem. Mat. 29 (2017) 5225-5231.
[12] S. Mandal, M. Rahaman, S. Sadhu, S. K. Nayak, A. Patra, Fluorescence Switching of Quantum Dot in Quantum Dot−Porphyrin−Cucurbit Uril Assemblies, J. Phys. Chem. C. 117 (2013) 3069−3077.
[13] O. Wang, L. Wang, Z. Li, Q. Xu, Q. Lin, H. Wang, Z. Du, H. Shen, L. S. Li, High-efficiency, deep blue ZnCdS/$Cd_xZn_{1-x}S$/ZnS quantum-dot-light-emitting devices with an EQE exceeding 18%, Nanoscale 10 (2018) 5650-5657.
[14] R.R. Banerjee, R. Jayakrishnan, P. Ayyub, Effect of the size-induced structural transformation on the band gap in CdS, J. Phys. 12 (50) (2000) 10647-10654.
[15] M.D. Regulacio, M.Y. Han, Composition Tunable alloyed Semiconductor Nanocrystals, Acc. Chem. Res. 43 (5) (2010) 621-630.
[16] X. Zhong, Y. Feng, W. Knoll, M. Han, Alloyed $Zn_xCd_{1-x}S$ nanocrystals with highly narrow luminescence spectral width, J. Am. Chem. Soc. 125 (2003) 13559-13563.
[17] Ch.Q. Wang, J.X. Xia, M. U. Ali, M. Liu, W. Lu, H. Meng, Facile synthesis of enhanced photoluminescent Mg:CdZnS/Mg:ZnS core/shell quantum dots, Mat. Sci. Proc. (2018) 96-102.
[18] J. Ouyang, C. I. Ratcliffe, D. Kingston, B. Wilkinson, J. Kuijper, X. Wu, J.A. Ripmeester, K. Yu, Gradiently alloyed $Zn_xCd_{1-x}S$ colloidal photoluminescent quantum dots synthesized via a noninjection one-pot approach, J. Phys. Chem. C. 112 (2008) 4908-4919.
[19] X. Jin, H. Li, S. Huang, X. Gu, H. Shen, D. Li, X. Zhang, Q. Zhang, F. Li, Q. Li, Bright alloy type-II quantum dots and their application to light-emitting diodes, J. Col. Inter. Sci. 510 (2018) 376-383.
[20] L. Loghina, M. Grinco, A. Iakovleva, S. Slang, K. Palka, M. Vlcek, Mechanistic investigation of the sulfur precursor evolution in the synthesis of highly photoluminescent $Cd_{0.15}Zn_{0.85}S$ quantum dots, New J. Chem. 42 (2018) 14779-14788.
[21] N. Sun, B. Li, J. Shao, W. Mo, B. Hu, Z. Shen, X. Hu, A general and facile one-pot process of isothiocyanates from amines under aqueous conditions, Beilstein J. Org. Chem. 8 (2012) 61-70.
[22] V.G. Klyuev, D.V. Volykhin, O.V. Ovchinnikov, S.I. Pokutnyi, Relationship between structural and optical properties of colloidal $Cd_xZn_{1-x}S$ quantum dots in gelatin, J. Nanophot. 10 (3) (2016) 033507(1-12).
[23] J.I. Langford, J.C. Wilson, Scherrer after sixty years: a survey and some new results in the determination of crystalline size, J. Appl. Crystallogr. 11 (1978) 102-113.
[24] M. Masab, H. Muhammad, F. Shah, M. Yasir, M. Hanif, Facile synthesis of CdZnS QDs: effects of different capping agents on the photoluminescence properties, Mat. Sci. Sem. Proc. 81 (2018) 113-117.
[25] N. C. Anderson, M. P. Hendricks, J. J. Choi, J. S. Owen, Ligand exchange and the stoichiometry of metal chalcogenide nanocrystals: Spectroscopic observation of facile

metal-carboxylate displacement and binding, J. Am. Chem. Soc. 135 (2013) 18536-18548.
[26] N.C. Anderson, J.S. Owen, Soluble, chloride-terminated CdSe nanocrystals: ligand exchange monitored by ^{1}H and ^{31}P NMR spectroscopy, Chem. Mater. 25 (2013) 69-76.
[27] S. Wageh, M. Maize, A.M. Donia, A.A. Al-Ghamdi, A. Umar, Synthesis and characterization of mercaptoacetic acid capped cadmium sulphide quantum dots, J. Nanosci. Nanotechnol. 15 (12) (2015) 9861-9867.
[28] W. Guo, N. Chen, C. Dong, Y. Tu, J. Chang, B. Zhang, One-pot synthesis of hydrophilic ZnCuInS/ZnS quantum dots for in vivo imaging, RSC Adv. 3 (2013) 9470-9475.
[29] J. K. Cooper, A. M. Franco, S. Gul, C. Corrado, J. Z. Zhang, Characterization of primary amine capped CdSe, ZnSe, and ZnS quantum dots by FT-IR: Determination of surface bonding interaction and identification of selective desorption, Langmuir 27 (2011) 8486–8493.
[30] M. Sun, H. Yu, W. YTang, L. Qi, F. Yang, X. Yang, Shape evolution of CdSe nanocrystals in vegetable oils: A synergistic effect of selenium precursor, Colloids and Surfaces A: Physicochem. Eng. Aspects 350 (2009) 91-100.
[31] Ch.V. Reddy, J. Shim, M. Cho, Synthesis, structural, optical and photocatalytic properties of CdS/ZnS core/shell nanoparticles, J. Phys. Chem. Sol. 103 (2017) 209-217.
[32] J.C. Bruce, N. Revaprasadu, K.R. Koch, Cadmium (II) complexes of N,N-diethyl-N'-benzoylthio(seleno)urea as a single-source precursors for the preparation of CdS and CdSe nanoparticles, New J. Chem. 31 (2007) 1647-1653.
[33] G.A. Reynolds, K.H. Drexhage, New coumarin dyes with rigidized structure for flashlamp-pumped dye lasers, Opt. Com. 13 (3) (1975) 222-224.
[34] J. Tauc, A. Menth, States in the gap, J. Non-Cryst. Sol. 8-10 (1972) 569-585.